Cancer Biol Med 2016. doi: 10.20892/j.issn.2095-3941.2016.0055

REVIEW

Multimodality imaging in nanomedicine and nanotheranostics

Xue Li[1,2], Xue-Ning Zhang[2], Xiao-Dong Li[2], Jin Chang[1]

[1]School of Life Sciences, Tianjin University, Tianjin Engineering Center of Micro-Nano Biomaterials and Detection-Treatment Technology, and Collaborative Innovation Center of Chemical Science and Engineering, Tianjin 300072, China; [2]Department of Radiology and Department of Radiation Oncology, Second Affiliated Hospital of Tianjin Medical University, Tianjin 300211, China

ABSTRACT Accurate diagnosis of tumors needs much detailed information. However, available single imaging modality cannot provide complete or comprehensive data. Nanomedicine is the application of nanotechnology to medicine, and multimodality imaging based on nanoparticles has been receiving extensive attention. This new hybrid imaging technology could provide complementary information from different imaging modalities using only a single injection of contrast agent. In this review, we introduce recent developments in multifunctional nanoparticles and their biomedical applications to multimodal imaging and theragnosis as nanomedicine. Most of the reviewed studies are based on the intrinsic properties of nanoparticles and their application in clinical imaging technology. The imaging techniques include positron emission tomography, single-photon emission computed tomography, computerized tomography, magnetic resonance imaging, optical imaging, and ultrasound imaging.

KEYWORDS Cancer nanomedicine; accurate diagnosis; tumor imaging; multimodal imaging; multifunctional nanoparticle

Introduction

Traditional clinical imaging techniques hardly meet the demands of individualized cancer diagnosis because of the growing trend toward the advancement of accurate diagnosis of diseases, especially cancer. These traditional techniques, such as positron emission tomography (PET), computed tomography (CT), X-ray, and magnetic resonance imaging (MRI), are hampered by impaired target specificity and limited information on the lesion location[1-3]. Nanocarrier-based molecular imaging systems, with their leaky tumor vasculature and poor lymphatic drainage, have received much attention to address these issues, because these systems provide an opportunity to enhance the target specificity for tumor tissue[2,4,5].

Nanoparticles are particulate materials with at least one dimension in the range of 1−100 nm. These particles have high surface-to-volume ratio, high surface energy, and unique mechanical, thermal, electrical, magnetic, and optical behaviors[6,7], which are not found in their bulk counterparts. These properties make the nanoparticles especially suitable for a wide range of applications in medicine. Nanomedicine involves the solution of various medical challenges and drawbacks faced by conventional medicine. These challenges include poor bioavailability, impaired target specificity, and systemic and organ toxicity[8]. Tumor tissues form leaky vasculatures and have poor lymphatic drainage around these tissues. Nanoparticles possess unique optical effect, electricity properties, and magnetic effects which has led to the extensive studies on the development of "nanoprobes" for molecular imaging. For example, superparamagnetic iron oxide (SPIO) and ultrasmall SPIO (USPIO) are used for MRI[9], gold nanoparticles for CT[10], quantum dots (QDs)[11] and upconversion nanoparticles (UCNPs)[12] for optical imaging, and carbon nanotubes and gold nanorods for photoacoustic contrast.

Much detailed information is highly needed for the accurate diagnosis of diseases. However, one single-imaging modality cannot provide complete information. PET, single-photon emission computed tomography (SPECT), and optical techniques, which produce images with detailed information, have high sensitivity but with poor resolution[13,14]. By contrast, X-ray, MRI, and CT can produce high-

Correspondence to: Jin Chang
E-mail: jinchang@tju.edu.cn
Received July 1, 2016; accepted August 25, 2016.
Available at www.cancerbiomed.org

resolution images of anatomy, but their sensitivity is relatively poor. Thus, the combination of imaging technologies has long been proposed. The first fused PET/CT instrument was developed in 1998 by Townsend et al. in collaboration with Siemens Medical. This instrument was considered one of the "Inventions of the Year" in 2000 by Time magazine[13], and this instrument became available commercially in 2001. Consequently, numerous multimodality imaging technologies have been designed and developed to boost the clinical benefits of hybrid imaging technology. In this review, we briefly introduce recent advances in multimodality imaging in nanomedicine and nanotheranostics.

Imaging technology and principal types of nanoparticles

Several examples of nanoparticles routinely used in imaging technology for nanomedical applications are liposomes, dendrimers, gold nanoparticle, QDs, iron oxide nanoparticle, nano-bubble, micelle, and mesoporous silica. Nanoparticles exhibit several advantages for imaging technology. Distinct intrinsic properties (e.g., electronic, optical, and magnetic properties) of nanoparticles could be easily tailored by controlling their phases, sizes, shapes, compositions, and surface characteristics to make them suitable for special functions for imaging. Additionally, the multicomponent nature of nanoparticles provides an extensive platform for combining two or multiple imaging modalities. The combined modalities exhibit great potential to overcome the limitations of a single imaging modality and provide more detailed information of the site through targeted delivery. In addition, a core–shell or a core–shell–shell (multiple shells)-type structure built hierarchically facilitates the incorporation of different therapeutic or diagnostic payloads in the core or different shells, making the nanoparticles suitable for multimodal applications. **Table 1** summarizes the most important applications, as well as the advantages and limitations, of these imaging techniques.

Multimodality imaging technologies based on PET

PET is an established routine clinical tool for whole-body imaging. This imaging technology need to utilize contrast agents containing positron-emitting radionuclide emitting pairs of γ-rays to generate imaging contrast[15]. The most frequently used radioactive contrast agents include ^{11}C, ^{13}N, ^{15}O, ^{18}F, ^{44}Sc, ^{62}Cu, ^{64}Cu, ^{68}Ga, ^{72}As, ^{74}As, ^{76}Br, ^{82}Rb, ^{86}Y, ^{89}Zr, and ^{124}I[16,17]. However, the small radionuclides are limited by their quick clearance efficiency and exposure of patients to high ionizing radiation. Compared with these radio atoms, nanoparticles has emerged as a new approach for PET imaging because of their improved biodistribution and target site accumulation of imaging contrast agents. Several studies have used nanoparticles to increase the number of radionuclides in each injection. For instance, Marik et al.[18] successfully prepared ^{18}F-labelled PEGylated liposomes and analyzed their biodistribution under the PET imaging format. Andreozzi et al.[19] labeled ^{64}Cu onto solid lipid nanoparticles using the chelator 6-[p-(bromoacetamido) benzyl]-1, 4, 8, 11-tetraazacyclotetradecane-N, N′, N″, N‴-tetraacetic acid (BAT). Moreover, the dose of contrast agents was decreased, while the ^{64}Cu units attached on nanoparticles.

However, γ-radiation is only weakly absorbed by the tissue, facilitating the imaging of organs deep inside the body.

Table 1 Overview, advantages, and limitations of the imaging techniques routinely used in nanomedicine research

Technique	Nanoparticles	Depth	Advantage	Limitation
PET/SPECT	Radio-labeled nanoparticles	No limit	Noninvasiveness and high sensitivity	Exposure to ionizing radiation and relatively low spatial resolution
CT	Gold, silver, and iodine nanoparticles	No limit	Noninvasiveness and high contrast resolution	Relatively high dose of ionizing radiation, limited soft tissue resolution, and exposure to ionizing radiation
MRI	Iron oxide nanoparticles, cobalt ferrites, and Gd^{3+}-labeled nanoparticles	No limit	Noninvasiveness and high spatial resolution	Relatively low sensitivity
Optical	Quantum dots	<1 cm	Noninvasiveness, and no harmful effect by nonionizing radiation	Relatively low spatial resolution
Ultrasound	Silica, nanobubble	Millimeters to centimeters	Noninvasiveness, real time, low cost, and no harmful effect by nonionizing radiation	Limited spatial resolution and unsuitable for examination of digestive organs and bone

Insufficient anatomical information and relatively low spatial resolution restrict the PET applicability *in vitro* and *in vivo* imaging. PET radio-labeled nanoparticles were prepared to provide a bifunctional imaging probe for a better application because of the multimodality of nanoparticle to perform several diagnostic functions in tandem. For example, Lee et al.[20] labeled ^{64}Cu on to the polyaspartic acid (PASP)-coated iron oxide (IO) to develop bifunctional IO nanoparticle probe for PET and MRI scans of tumor integrin αvβ3 expression (**Figure 1A** and **B**). Small-animal PET and T2-weighted MRI showed integrin-specific delivery of conjugated RGD-PASP-IO nanoparticles and prominent reticuloendothelial system uptake. In another case, PET imaging was integrated with luminescence imaging by direct incorporation of ^{64}Cu into CuInS/ZnS nanoparticles[21] (**Figure 1C** and **D**). The as-prepared bimodal probes were intravenously injected into U87MG mouse xenograft model via the tail vein. Consequently, high tumor uptake (10.8% ID/g) of [^{64}Cu]CuInS/ZnS QDs was found, and the efficient PET/self-illuminating luminescence bio-model imaging was identified. This combination successfully resolved the lack of quantitation and shallow depth of penetration of the fluorophore probes. The dose of the radio atoms was efficiently reduced, improving their biosecurity.

Multimodality imaging technologies based on SPECT

SPECT is an imaging technique based on noncoincident γ-rays generated by radionuclides. Commonly used radioisotopes for SPECT are ^{99m}Tc, ^{111}In, ^{123}I, ^{125}I, and ^{201}Tl. Analogous to PET, the most important advantages of SPECT are its sensitivity and high penetration depth, whereas its disadvantages include lack of anatomical information and relatively low spatial resolution. SPECT is usually combined with structural imaging technique, such as CT and MRI. Among these multimodal techniques, imaging pattern of SPECT/CT has received much attention for incorporating a nanoparticle. An example is a liposomal nanocarrier conjugated with ^{99m}Tc to form nano-probe for SPECT/CT imaging[22]. This imaging pattern was used to visualize and quantify drug delivery to tumors, and the therapeutic effects of this technique were analyzed. Nude mice injected with head-and-neck squamous cell carcinoma xenografts on both sides of the skull base for approximately 5 min were treated with radio frequency ablation (RFA). RFA substantially increased the tumor accumulation of radio-labeled liposomal doxorubicin. Moreover, the results evidently showed that SPECT/CT could depict the state of tumor with higher sensitivity than single imaging pattern. Arranja et al.[23] employed SPECT/CT to assess the biodistribution of pluronic-based nanocarriers with different PEO block lengths and aggregation states *in vivo* using ^{111}In-radiolabeled pluronic nanocarriers. Their results successfully revealed different renal and liver clearances with various polyoxyethylene block length or aggregation state of the copolymers.

SPECT is suitable for monitoring the pharmacokinetics, biodistribution, and target site accumulation because of their imaging sensitivity and penetration depth. However, relatively more difficult quantification seriously hampers this application. Thus, except for combined CT or MRI to improve anatomical information and spatial resolution, optical imaging is usually added to further overcome the limitations of individual imaging to obtain more detailed information on the lesion location. Studies have integrated SPECT, MR, and optical imaging modalities by encapsulating Gd_2O_3 cores within a polysiloxane shell, which carries organic fluorophore (Cy 5) and is derivatized by a hydrophilic carboxylic layer (**Figure 2**). Well-prepared multimodal imaging agents were used to evaluate the biodistribution of these multimodal nanoparticles in rodents. Comprehensive analysis of the results of MR imaging, optical fluorescent imaging, and SPECT evidently confirmed the quantitative biodistribution and pharmacokinetics of multimodal nanoscale agents[24].

Multimodality imaging technologies based on CT

X-ray CT is one of the most common imaging methods that uses computer-processed X-ray scans to produce tomographic images of a specific area of the body[25]. High-contrast images and distinct anatomical visualization of several tissues, such as blood vessels, stomach, and gastrointestinal organs, could be obtained because of the inherent distinctions in X-ray absorption and attenuation by different components of the body. By contrast, soft tissues with similar inherent CT contrast cannot be distinguished clearly[26,27]. Consequently, CT contrast agents with large atomic weight (high Z) elements are usually required to better delineate regions of interest. Several common contrast agents are iodine (nonradioactive), gold, platinum, bismuth, tantalum, and ytterbium. However, these contrast agents are excreted rapidly through the kidney after administration, allowing only short imaging periods. High Z element-containing nanoparticle contrast agents for CT, especially CT-based multimodal imaging, have been extensively

explored in the past decade, because the nanoparticles can extend circulation lifetime and enhance the aggregation at the regions of interest[28, 29].

Majority of the studies have explored gold nanostructures

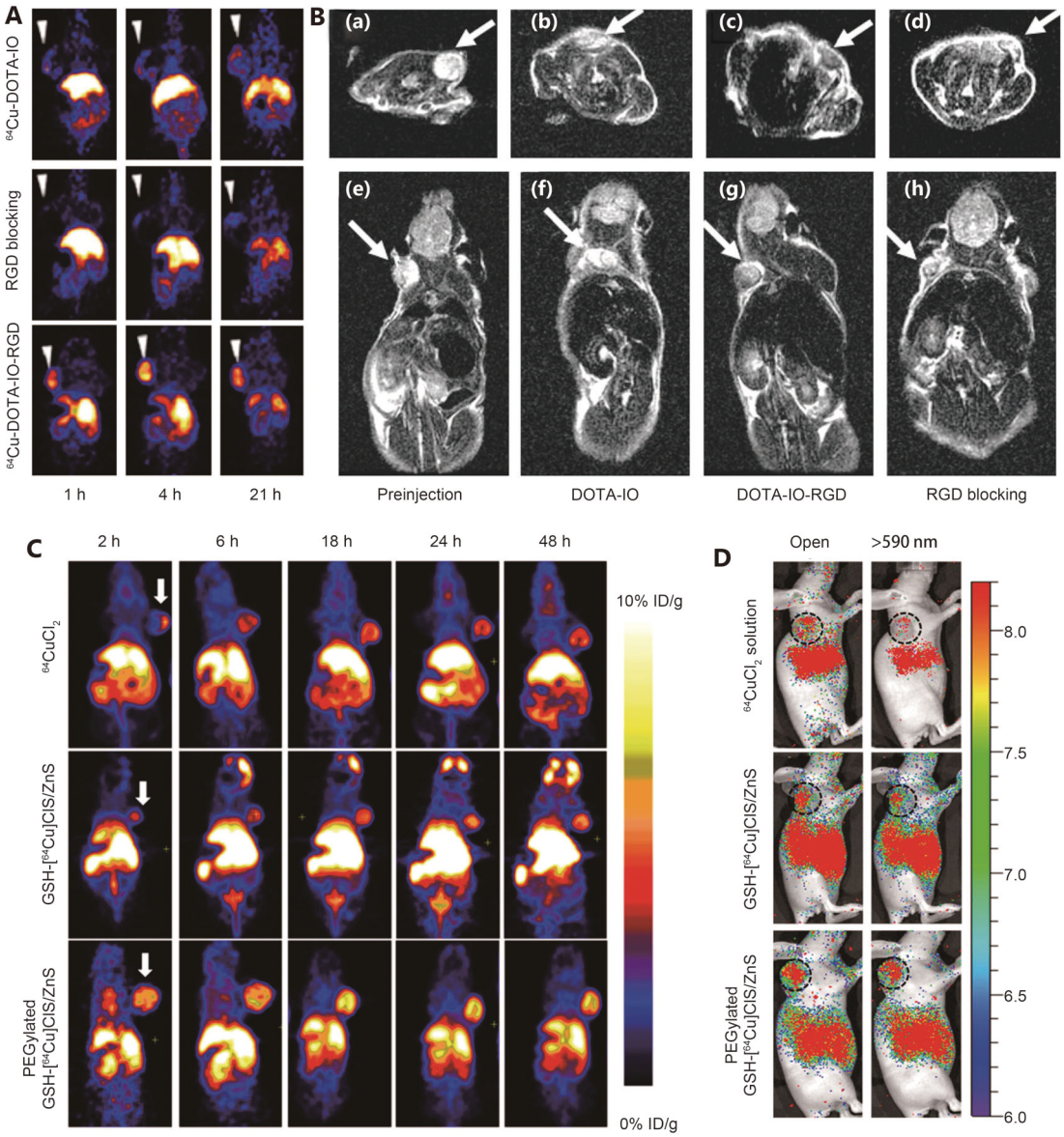

Figure 1 (A) Decay-corrected whole-body coronal positron electron tomographic images of nude mice bearing human U87MG tumor at 1, 4, and 21 h after injection of 3.7 MBq of ^{64}Cu-DOTA-IO, ^{64}Cu-DOTA-IO-RGD, or ^{64}Cu-DOTA-IO-RGD with 10 mg of c(RGDyK) peptide per kilogram (300 μg of iron-equivalent IO particles per mouse). (B) T2-weighted magnetic resonance images of nude mice bearing U87MG tumor before injection of IO nanoparticles (a, e) and at 4 h after tail-vein injection of DOTA-IO (b, f), DOTA-IO-RGD (c, g), and DOTA-IO-RGD with blocking dose of c(RGDyK) (d, h). Reproduced with permission from, Ref. 20. Copyright 2008 Society of Nuclear Medicine and Molecular Imaging. (C) Representative whole-body coronal positron electron tomographic images of U87MG tumor-bearing mice at 2, 6, 18, 24, and 48 h after intravenous (IV) injection of 100 μL (50 μg, 300 μCi) of $^{64}CuCl_2$, GSH-[^{64}Cu]CIS/ZnS, and PEGylated GSH-[^{64}Cu]CIS/ZnS RQDs (3 mice per group). (D) CRET images of U87MG tumor-bearing mice at 6 h after injection of 100 μL (300 μCi) of $^{64}CuCl_2$, GSH-[^{64}Cu]CIS/ZnS, and PEGylated GSH-[^{64}Cu]CIS/ZnS RQDs, respectively. Circle, tumor area (3 mice per group). These luminescence images were acquired without excitation light with open and red filter (>590 nm). Reproduced with permission from Ref. 21. Copyright 2014 American Chemical Society.

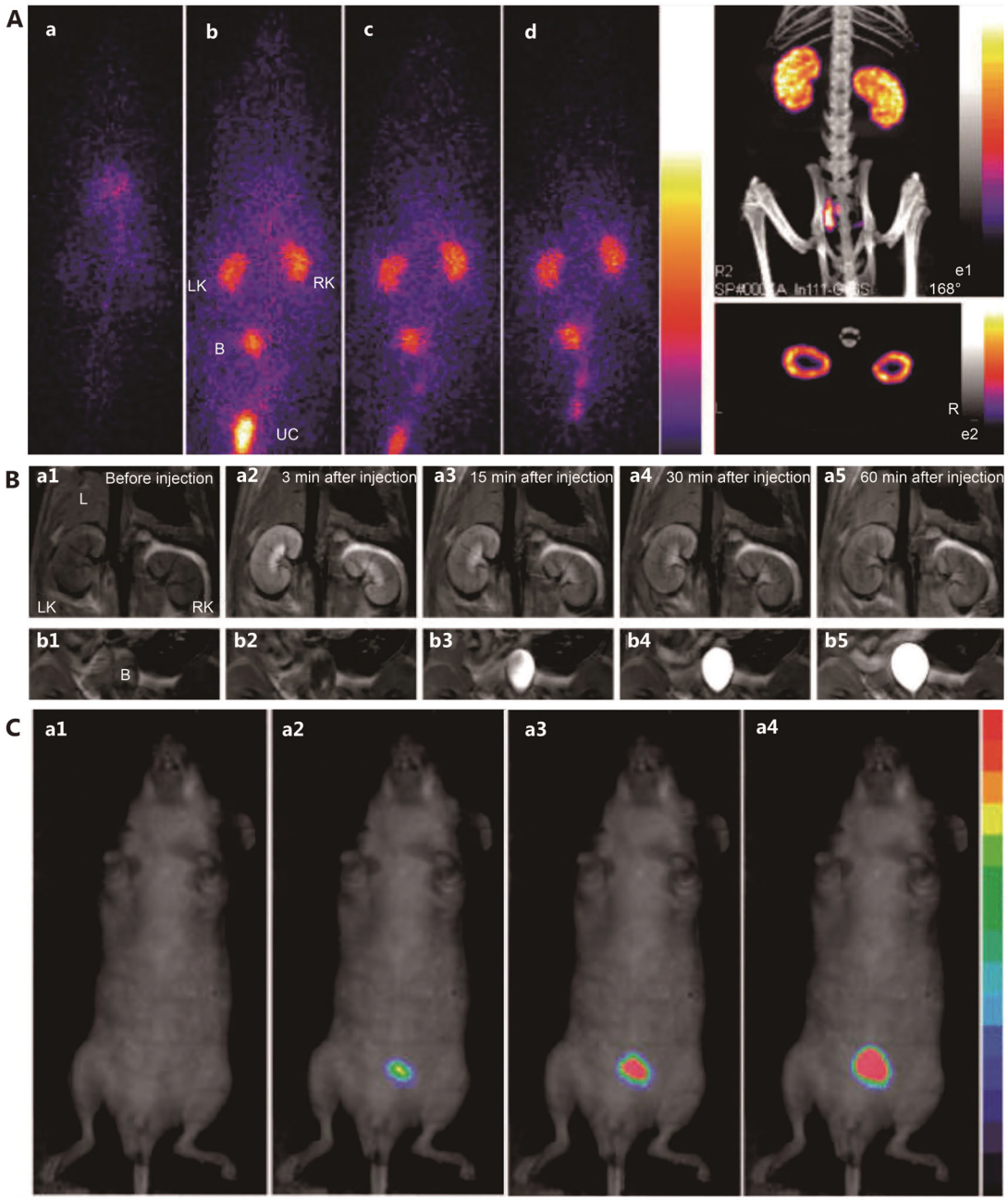

Figure 2 (A) SPECT/CT *in vivo* imaging in Wistar rats. Planar sequential scintigraphic images acquired during IV injection of 25 MBq of Gado-^{6}Si-NP_^{111}In (a) and at 15 (b), 30 (c), and 60 min (d) after injection. Tomographic scintigraphy and X-ray CT of the whole body of the rat acquired at day 2, posterior projection (e1) and transversal slice (e2). LK: left kidney. RK: right kidney. B: bladder. UC: urine collector. (B) T1w.seq. Coronal images acquired before and at 3, 15, 30, and 60 min after IV injection of 50 µL of Gado-6Si-NP, centered on kidneys (a) and bladder (b). (C) Ventral (a1, 2, 3, and 4) and dorsal (b1, 2, 3, and 4) planar fluorescence reflectance images acquired at the end of IV injection of Gado-^{6}Si-NP (a1, b1), at 15 (a2, b2), 30 (a3, b3), and 60 min (a4, b4) after injection. Reproduced with permission from Ref. 24. Copyright 2011 American Chemical Society.

because of their high X-ray attenuation coefficient and biocompatibility. Thus, gold nanoparticle-containing multiple contrast agents were developed for simultaneous use in different imaging modalities (e.g., PET, SPECT, MRI, and optical imaging). Compared with PET/CT imaging, PET/MRI provides better contrast of anatomical imaging of

either hard or soft tissues with excellent sensitivity. In one example, Gd chelates, which are the commonly used MRI modalities, were used to decorate the surface of gold nanoparticle to combine CT and MRI (**Figure 3A**)[30]. Radiotherapy procedures guided by both CT and MR imaging are desirable, because they present the benefits of the two bio-imaging models. In these procedures, CT is used to perform radiation dose mapping, whereas MRI provides soft tissue contrast to identify target tissues. The use of a hybrid probe allows co-registration without the use of invasive fiducial markers.

Nanoparticle platforms also facilitate the exploration of other materials, such as bismuth sulfide, nanoparticles, for a new-generation CT imaging agent[31,32]. Gao and Chai prepared sub-10 nm Bi_2S_3 biocompatible particles coated with bovine serum albumin for multimodal imaging (CT/PET/PA imaging) (**Figure 3B**). Prolonged circulation time *in vivo* was observed after IV administration in rats. Different combinations of treatments are applied to evaluate the performance of as-prepared Bi_2S_3 NPs in photothermal and radiotherapy of tumors with the guidance of multimodal imaging. Thus, the implanted tumors are completely eradicated through combined therapies and visualized with combined CT/PET/PA imaging contrast[33].

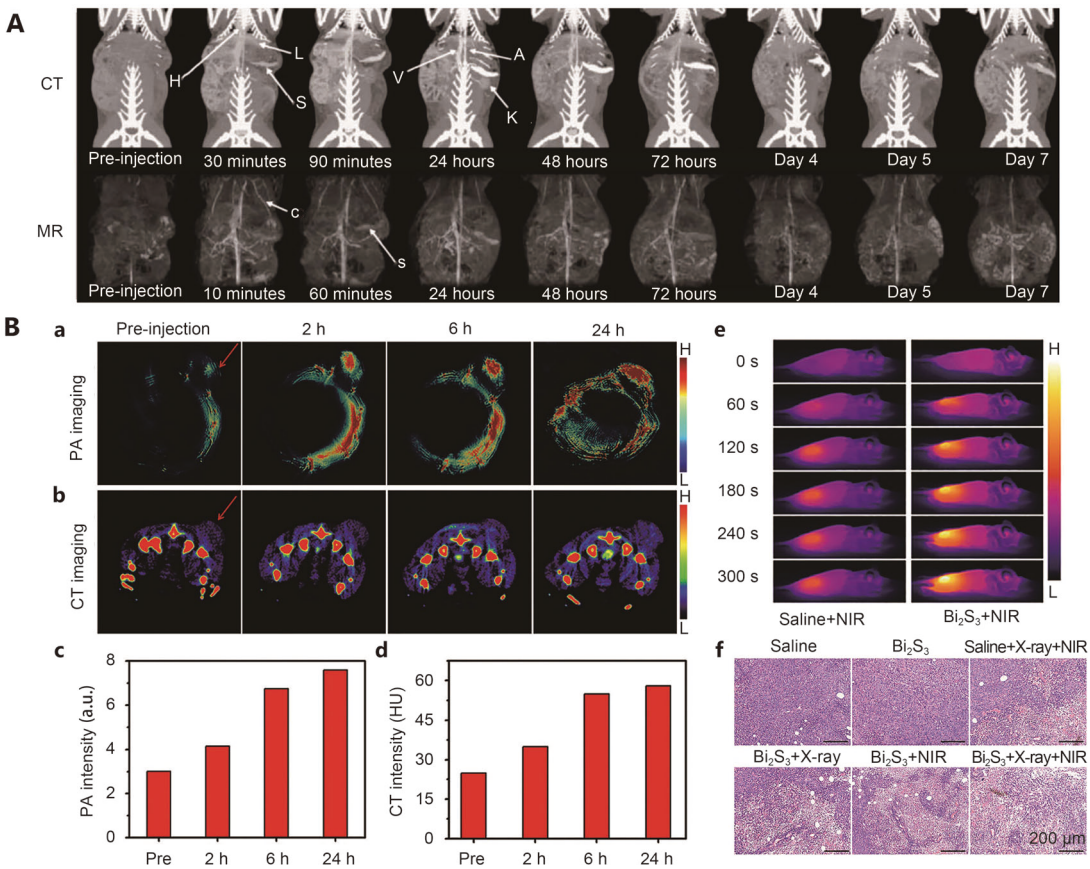

Figure 3 (A) Three-dimensional maximum intensity projection images (anterior view) of a healthy New Zealand white rabbit (3 kg) obtained in CT (120 kV, 200 mA) and MR (3D FSPGR sequence, TR/TE=9.8/4.3) prior to and after IV administration (as indicated) of the liposome formulation of iohexol and gadoteridol. Reproduced with permission from Ref. 30. Copyright 2007 Springer. (B) *In vivo* PA images (a) and PA signal intensities (c) of the tumorous area recorded at 0, 2, 6, and 24 h after IV injection of Bi_2S_3 NPs into mice bearing 4 T1 tumors (dosage: 200 μL of Bi_2S_3 NPs solution containing 0.5 mg Bi). *In vivo* CT images (b) and signal intensities (d) of the tumorous area of another group of tumor-bearing mice recorded at 0, 2, 6, and 24 h after IV injection of Bi_2S_3 NPs (dosage: 200 μL of Bi_2S_3 NPs containing 1 mg Bi). The tumor site is pointed by red arrows. e: Infrared thermal images of tumor-bearing mice recorded during laser irradiation. f: H&E staining of tumor tissues harvested from the different groups of mice. Reproduced with permission from Ref. 33. Copyright 2016 Wiley-VCH Verlag GmbH &Co. KGaA, Weinheim.

Multimodality imaging technologies based on MRI

MRI is the most popular clinically applied examination method based on nuclear magnetic resonance, which typically depends on the spin–lattice relaxation and the spin–spin relaxation time of protons contained in different tissues or organs to create imaging contrast[34,35]. MRI could provide excellent anatomic detail, enhanced soft tissue contrast, high spatial resolution, and no radiation exposure. Thus, MRI plays an increasing role in clinical diagnosis[35]. However, this process is limited by insufficient signal sensitivity, resulting in low contrast in small or tiny tumor diagnosis. Thus, nanoparticles with magnetic functionality is recently widely explored to enhance the MRI detection sensitivity and accuracy. Paramagnetic ions, such as manganese (Mn^{2+}), iron (Fe^{3+}), and gadolinium (Gd^{3+}), are usually used to provide MRI contrast. Among these ions, Gd^{3+} units are the most common T1 contrast agents directly attached near the nanoparticle surface to affect T1 relaxation time of protons. SPIOs, which reduce the spin–spin relaxation time of proton, are regarded as the intrinsic T2 contrast agent[36,37]. Moreover, SPIOs have been used in preclinical and clinical MRI[38,39] because of their effect on the reticuloendothelial system (RES) and nontoxicity in biological systems. These nanoparticles can be co-incorporated with other imaging nanoparticles or covered with small imaging molecule to combine two or more imaging format[40]. For instance, Zhou et al.[41] reported Gd-embedded iron oxide (GdIO) nanoparticles to acquire both T1 and T2 enhanced contrast agents. These nanoparticles simultaneously improve T1 and T2 to increase the conspicuity of MRI by enhancing the contrast in the regions of interest with bright and dark signals, respectively. Thus, improved diagnostic results were obtained (**Figure 4A**).

PET (or SPECT) and fluorescent imaging were also coupled with MRI to provide extremely sensitive and high-resolution images. Otherwise, CT can improve temporal resolution of MRI[42,43]. Mitchell et al.[44] group designed a series of metal-chelating lipid conjugates chelated to Gd^{3+}, $^{64}Cu^{2+}$, or $^{111}In^{3+}$. Then, they prepared liposomes incorporating the conjugates to integrate the function of MR and SPECT, even fluorescence. The hybrid system had been proved to overcome the sensitivity difference between MRI and SPECT *in vivo*. In another example, a multimodality imaging contrast agent was employed to tumor angiogenesis imaging[45]. Studies have designed a lanthanide-based nanoprobe using NaLuF4:Yb, Tm as the core and 4 nm of 153Sm3þ-doped NaGdF4 (half-life of 153Sm = 46.3 h) as the shell, and a lanthanide-based core shell nanocomposite for an optimized multimodal imaging probe with enhanced imaging ability. The NIR fluorescence, CT, MRI, and PET were simultaneously used for tumor angiogenesis imaging in mice (**Figure 4B**).

Multimodality imaging technologies based on optical imaging

Compared with other imaging techniques, optical imaging has numerous unique advantages, such as simplicity of use, simultaneous detection of multiple markers, and wide spatial scales ranging from subcellular structures to tissues. This imaging format is commonly used in biological experiments[46], fluorescence-guided surgery, and endoscopic imaging[47]. However, the limitation of penetration hinders the development of optical imaging technologies.

Eleven QDs exhibit high quantum yield, broad absorption spectra, narrow tunable emission spectra, excellent photostability, and chemical stability. These QDs has been regarded as novel optical probes for medicine. Encapsulating magnetic nanoparticles and quantum dots is one of the major methods to obtain multimode nanocomposites for imaging. For example, PLGA is used as the template to encapsulate QDs and iron oxide nanoparticles and form the double modal imaging agent[48]. In this case, the QDs enable optical imaging, whereas iron oxide nanoparticles are used for magnetic targeting and MRI contrast agents. The ratio and density of these two nanoparticles embedded within the polymer can be easily controlled.

UCNPs have recently attracted great attention as a new generation of optical imaging probe[49]. Contrary to conventional fluorophores, UCNPs emit higher-energy visible light when excited by NIR light. Moreover, various multifunctional UCNPs could be obtained by varying their compositions. For example, UCNPs with Gd^{3+} and ^{18}F could be used for MRI and PET[50,51], while UCNP with lanthanide component could be used as a CT contrast agent[52].

Multimodality imaging technologies based on ultrasound (US) imaging

US imaging is based on the difference in the ultrasound passage rate through tissues, allowing real-time imaging during operation and pre-surgical planning because of their cost effectiveness and safety. However, this imaging technique is limited by relatively low resolution, sensitivity, and penetration. Microbubbles are currently used as US contrast agents. Additionally, nanoscale liquid–liquid

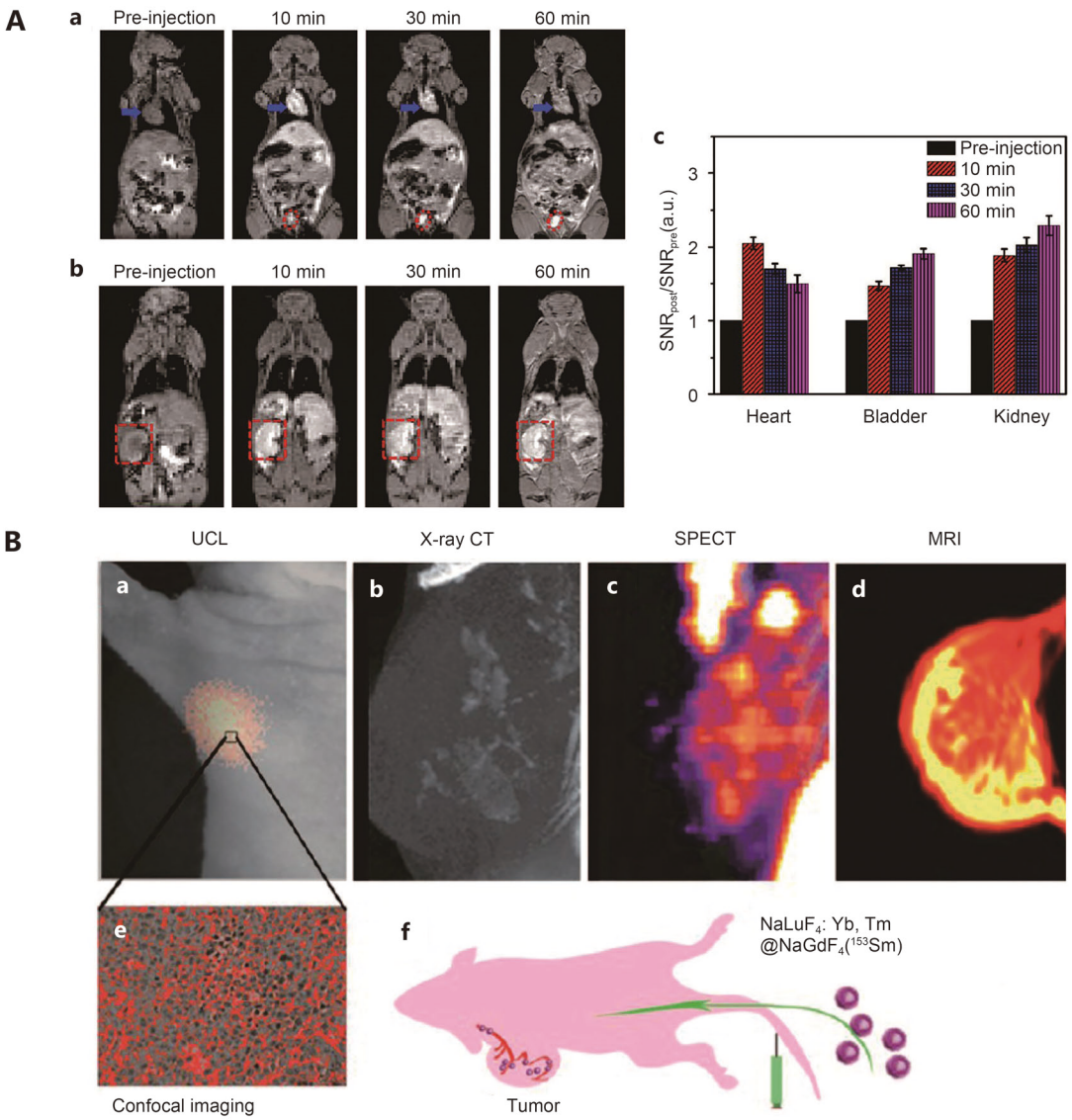

Figure 4 (A) *In vivo* T1 MR imaging and analysis of mice after intravenous injection of 4.8 nm GdIO@ZDS nanoparticles as contrast agents. a, b: MR images of mice after tail vein injection of 4.8 nm GdIO@ZDS nanoparticles (2.0 mg/kg) at 0, 10, 30, and 60 min, respectively. Blue arrows show the heart, red dot circles show the bladder, and the red dashed squares indicate the kidney. c: Quantification of signal changes (SNR ratio) in the heart, bladder, and kidney at different time points after administration (n=3). Reproduced with permission from Ref. 41. Copyright 2013 American Chemical Society. (B) a-d: Four-modal imaging of the focused tumor from the tumor-bearing nude mouse 1 h after IV injection of $NaLuF_4$: Yb, Tm@$NaGdF_4$ (^{153}Sm). a: *In vivo* UCL. b: X-ray CT. c: SPECT. d: MR images of the tumor. e: UCL confocal image of the paraffin section of tumor tissue. (f) Schematic illustration of tumor angiogenesis imaging using $NaLuF_4$:Yb,Tm@$NaGdF_4$ (^{153}Sm) as the probe. Reproduced with permission from Ref. 44. Copyright 2013 American Chemical Society.

emulsions, gas–liquid emulsions, and solid nanoparticles have also been reported to contribute to enhance contrast of US imaging[53]. The major multimodal format for US is its combination with MRI contrast agent. PLGA was used as the stabilizer to encapsulate nanoparticles and chemotherapeutic drugs. This hybrid imaging agent reveals the contrast in MRI and US, and US-triggered chemotherapeutic drug release[54].

Conclusions

In this review, we discussed how nanotechnology facilitates the combination of different imaging agents to one hybrid

material and their preliminary application for tumor diagnosis. These promising imaging contrast agents could provide complementary information from different imaging modalities using only a single injection of contrast agents, providing detailed information of a disease. However, most of the reported studies only used animal models, and clinical studies are rarely performed. Further studies are necessary before any of these nanoparticle agents could be applied clinically.

The following aspects should be considered for effective clinical translation. First, targeted delivery of imaging agents (e.g. molecular recognition) should be paid more attention to determine the effect of the specificity of targeting and potential toxic side effect caused by off-target accumulation of active agents. Second, these new generation imaging agents are composed of materials with low toxicity or high biodegradability (e.g., biodegradable silicon QDs). Third, more efficient nanocarriers should be developed for externally controlled release of nanoparticles for accurate diagnosis.

Conflict of interest statement

No potential conflicts of interest are disclosed.

References

1. Jokerst JV, Gambhir SS. Molecular imaging with theranostic nanoparticles. Acc Chem Res. 2011; 44: 1050-60.
2. Wang D, Lin B, Hua A. Theranostic nanoparticles for cancer and cardiovascular applications. Pharm Res. 2014; 31: 1390-406.
3. Wang W, Tao N. Detection, counting, and imaging of single nanoparticles. Anal Chem. 2013; 86: 2-14.
4. Kunjachan S, Ehling J, Storm G, Kiessling F, Lammers T. Noninvasive imaging of nanomedicines and nanotheranostics: principles, progress, and prospects. Chem Rev. 2015; 115: 32-48.
5. Villanueva MT. Imaging in oncology: lighting the way. Nat Rev Clin Oncol. 2012; 667: 208-8.
6. Burda C, Chen X, Narayanan R, El-Sayed MA. Chemistry and properties of nanocrystals of different shapes. Chem Rev. 2005; 105: 1025-102.
7. Chen G, Roy I, Yang C, Prasad PN. Nanochemistry and nanomedicine for nanoparticle–based diagnostics and therapy. Chem Rev. 2016; 116: 2826-85.
8. Riehemann K, Schneider SW, Luger TA, Godin B, Ferrari M, Fuchs H, Nanomedicine–challenge and perspectives. Angew Chem Int Ed. 2009; 48: 872-97.
9. Wang X, Xing X, Zhang B, Liu F, Cheng Y, Shi D. Surface engineered antifouling optomagnetic SPIONs for bimodal targeted imaging of pancreatic cancer cells. Int J Nanomedicine. 2014; 9: 1601-15.
10. Yan D, Guo Y, Li X, Xue L, Sheng W, Lin W, et al. Size-tuning ionization to optimize gold nanoparticles for simultaneous enhanced CT imaging and radiotherapy. ACS Nano. 2016; 10: 2536-48.
11. Guo W, Chen N, Dong C, Tu Y, Chang J, Zhang B. One-pot synthesis of hydrophilic ZnCuInS/ZnS quantum dots for in vivo imaging. Rsc Adv. 2013; 3: 9470-75.
12. Zheng B, Su L, Pan H, Hou B, Zhang Y, Zhou F, et al. NIR-remote selected activation gene expression in living cells by upconverting microrods. Adv Mater. 2015; 28: 707-14.
13. Louie A. Multimodality imaging probes: design and challenges. Chem Rev. 2010; 110: 3146-95.
14. Ali Z, Abbasi AZ, Zhang F, Arosio P, Lascialfari A, Casula MF, et al. Multifunctional nanoparticles for dual imaging. Anal Chem. 2011; 83: 2877-82.
15. Shokeen M, Fettig NM, Rossin R. Synthesis, in vitro and in vivo evaluation of radiolabeled nanoparticles. Q J Nucl Med Mol Imaging. 2008; 52: 267-77.
16. Bar Shalom R, Valdivia AY, Blaufox MD. PET imaging in oncology. Semin Nucl Med. 2000; 30: 150-85.
17. Adam MJ, Wilbur DS. Radiohalogens for imaging and therapy. Chem Soc Rev. 2005; 36: 153-63.
18. Marik J, Tartis MS, Zhang H, Fung JY, Kheirolomoom A, Sutcliffe JL, et al. Long–circulating liposomes radiolabeled with [^{18}F]fluorodipalmitin ([^{18}F]FDP). Nucl Med Biol. 2007; 34: 165-71.
19. Andreozzi E, Seo JW, Ferrara K, Louie A. Novel method to label solid lipid nanoparticles with ^{64}Cu for positron emission tomography imaging. Bioconjug Chem. 2011; 22: 808-58.
20. Lee HY, Li Z, Chen K, Hsu AR, Xu C, Xie J, et al. PET/MRI dual-modality tumor imaging using arginine–glycine-aspartic (RGD)-conjugated radiolabeled iron oxide nanoparticles. J Nucl Med. 2008; 49: 1371-79.
21. Guo W, Sun X, Orit J, Yan X, Min K, Srivatsan A, et al. Intrinsically radioactive [^{64}Cu]CuInS/ZnS quantum dots for PET and optical imaging: improved radiochemical stability and controllable cerenkov luminescence. ACS Nano. 2015; 9: 488-95.
22. Head HW, Bao A, Soundararajan A, Garcia Rojas X, Prihoda TJ, McManus LM, et al. Combination radiofrequency ablation and intravenous radiolabeled liposomal Doxorubicin: imaging and quantification of increased drug delivery to tumors. Radiology. 2010; 13: 32-53.
23. Arranja A, Ivashchenko O, Denkova AG, Morawska K, van Vlierberghe S, Dubruel P, et al. SPECT/CT imaging of pluronic nanocarriers with varying poly(ethylene oxide) block length and aggregation State. Mol Pharm. 2016; 13: 1158-65.
24. Kryza D, Taleb J, Janier M, Marmuse L, Miladi I, Bonazza P, et al. Biodistribution study of nanometric hybrid gadolinium oxide particles as a multimodal SPECT/MR/optical imaging and theragnostic agent. Bioconjug Chem. 2011; 22: 1145-52.
25. Liu Y, Ai K, Lu L. Nanoparticulate X–ray computed tomography contrast agents: from design validation to in vivo applications. Acc Chem Res. 2012; 45: 1817-27.
26. Sakuma S, Takeuchi T, Ishigaki T. X-ray computed tomography. Physics Education. 2001; 36: 442-51.
27. Krause W, Schneider PW. Chemistry of X–ray contrast agents. Top Curr Chem. 2002; 222: 107-50.

28. Zhu J, Lu Y, Li Y, Jiang J, Cheng L, Liu Z, et al. Synthesis of Au-Fe3O4 heterostructured nanoparticles for in vivo computed tomography and magnetic resonance dual model imaging. Nanoscale. 2014; 6: 199-202.
29. JLL, DAF, MBS, Peter Schiffer A, Williams ME. Synthesis of Fe oxide core/Au shell nanoparticles by iterative hydroxylamine seeding. Nano Lett. 2004; 4: 719-23.
30. Zheng J, Liu J, Dunne M, Jaffray DA, Allen C. In vivo performance of a liposomal vascular contrast agent for CT and MR–based image guidance applications. Pharm Res. 2007; 24: 1193-201.
31. Ai K, Liu Y, Liu J, Yuan Q, He Y, Lu L. Large-scale synthesis of Bi2S3 nanodots as a contrast agent for in vivo X-ray computed tomography imaging. Adv Mater. 2011; 23: 4886-891.
32. Wang S, Li X, Chen Y, Cai X, Yao H, Gao W, et al. A facile one–pot synthesis of a two–dimensional MoS_2/Bi_2S_3 composite theranostic nanosystem for multi-modality tumor imaging and therapy. Adv Mater. 2015; 27: 2775-82.
33. Wang Y, Wu Y, Liu Y, Shen J, Lv L, Li L, et al. BSA–mediated synthesis of bismuth sulfide nanotheranostic agents for tumor multimodal imaging and thermoradiotherapy. Adv Funct Mater. 2016; 26: 5335-44.
34. Kircher MF, Willmann JK. Molecular body imaging: MR imaging, CT, and US. part I. principles. Radiology. 2012; 263: 633-43.
35. Willmann JK, Bruggen NV, Dinkelborg LM, Gambhir SS. Molecular imaging in drug development. Nat Rev Drug Discov. 2008; 7: 591-607.
36. Ling D, Lee N, Hyeon T. Chemical synthesis and assembly of uniformly sized iron oxide nanoparticles for medical applications. Acc Chem Res. 2015; 48: 1276-85.
37. Corot C, Robert P, Idée JM, Port M. Recent advances in iron oxide nanocrystal technology for medical imaging. Adv Drug Deliv Rev. 2006; 58: 1471-504.
38. Hagspiel KD, Neidl KF, Eichenberger AC, Weder W, Marincek B. Detection of liver metastases: comparison of superparamagnetic iron oxide-enhanced and unenhanced MR imaging at 1.5 T with dynamic CT, intraoperative US, and percutaneous US. Radiology. 1995; 196: 471-78.
39. Li W, Tutton S, Vu AT, Pierchala L, Li BS, Lewis JM, et al. First-pass contrast-enhanced magnetic resonance angiography in humans using ferumoxytol, a novel ultrasmall superparamagnetic iron oxide (USPIO)-based blood pool agent. J Magn Reson Imaging. 2005; 21: 46-52.
40. Shin TH, Choi JS, Yun S, Kim IS, Song HT, Kim Y, et al. T1 and T2 dual-mode MRI contrast agent for enhancing accuracy by engineered nanomaterials. ACS Nano. 2014; 8: 3393-401.
41. Zhou Z, Wang L, Chi X, Bao J, Yang L, Zhao W, et al. Engineered iron-oxide-based nanoparticles as enhanced T1 contrast agents for efficient tumor imaging. ACS Nano. 2013; 7: 3287-96.
42. Yang X, Hong H, Grailer JJ, Rowland IJ, Javadi A, Hurley SA, et al. cRGD-functionalized, DOX-conjugated, and ^{64}Cu–labeled superparamagnetic iron oxide nanoparticles for targeted anticancer drug delivery and PET/MR imaging. Biomaterials. 2011; 32: 4151-60.
43. Hagit A, Soenke B, Johannes B, Shlomo M. Synthesis and characterization of dual modality (CT/MRI) core-shell microparticles for embolization purposes. Biomacromolecules. 2010; 11: 1600-7.
44. Mitchell N, Kalber TL, Cooper MS, Sunassee K, Chalker SL, Shaw KP, et al. Incorporation of paramagnetic, fluorescent and PET/SPECT contrast agents into liposomes for multimodal imaging. Biomaterials. 2012; 34: 1179-92.
45. Sun Y, Zhu X, Peng J, Li F. Core–shell lanthanide upconversion nanophosphors as four–modal probes for tumor angiogenesis imaging. ACS Nano. 2013; 7: 11290-300.
46. Wu X, Liu H, Liu J, Haley KN, Treadway JA, Larson JP, et al. Immunofluorescent labeling of cancer marker Her2 and other cellular targets with semiconductor quantum dots. Nat Biotechnol. 2003; 21: 41-6.
47. Nguyen QT, Tsien RY. Fluorescence-guided surgery with live molecular navigation-a new cutting edge. Nat Rev Cancer. 2013; 13: 653-62.
48. Kim J, Lee JE, Lee SH, Yu JH, Lee JH, Park TG, et al. Designed fabrication of a multifunctional polymer nanomedical platform for simultaneous cancer-targeted imaging and magnetically guided drug delivery. Adv Mater. 2008; 20: 478-83.
49. Chatterjee DK, Gnanasammandhan MK, Zhang Y. Small upconverting fluorescent nanoparticles for biomedical applications. Small. 2010; 6: 2781-95.
50. Liu Q, Sun Y, Li C, Zhou J, Li C, Yang T, et al. ^{18}F-Labeled magnetic-upconversion nanophosphors via rare-earth cation-assisted ligand assembly. ACS Nano. 2011; 5: 3146-57.
51. Meng H, Peng H, Zhang C, Hu H, Bao C, Guo Gao, et al. Dual phase-controlled synthesis of uniform lanthanide-doped $NaGdF_4$ upconversion nanocrystals via an OA/ionic liquid two-phase system for in vivo dual-modality imaging. Adv Funct Mater. 2011; 21: 4470-7.
52. Ke H, Wang J, Dai Z, Jin Y, Qu E, Xing Z, et al. Gold–nanoshelled microcapsules: a theranostic agent for ultrasound contrast imaging and photothermal therapy. Angew Chem Int Ed Engl. 2011; 50: 3017-21.
53. Meng H, Peng H, Zhang C, Hu H, Bao C, Guo Gao, et al. Dual phase-controlled synthesis of uniform lanthanide-doped $NaGdF_4$ upconversion nanocrystals via an OA/ionic liquid two-phase system for in vivo dual-modality imaging. Adv Funct Mater. 2011; 21: 4470-7.
54. Niu C, Wang Z, Lu G, Krupka TM, Sun Y, You Y, et al. Doxorubicin loaded superparamagnetic PLGA-iron oxide multifunctional microbubbles for dual-mode US/MR imaging and therapy of metastasis in lymph nodes. Biomaterials. 2013; 34: 2307-17.

Cite this article as: Li X, Zhang X, Li X, Chang J. Multimodality imaging in nanomedicine and nanotheranostics. Cancer Biol Med. 2016; 13: 339-48. doi: 10.20892/j.issn.2095-3941.2016.0055